Article

Synthesis of C3-symmetric cinchona-based organocatalysts and their application in asymmetric Michael and Friedel–Crafts reactions

Péter Kisszékelyi [1,*], Zsuzsanna Fehér [1], Sándor Nagy [1], Péter Bagi [1], Petra Kozma [1], Zsófia Garádi [2,3], Miklós Dékány [4], Péter Huszthy [1], Béla Mátravölgyi [1], and József Kupai [1,*]

[1] Department of Organic Chemistry & Technology, Budapest University of Technology & Economics, Szent Gellért tér 4, H-1111 Budapest, Hungary

[2] Department of Inorganic & Analytical Chemistry, Budapest University of Technology & Economics, Szent Gellért tér 4, H-1111 Budapest, Hungary

[3] Department of Pharmacognosy, Semmelweis University, Üllői út 26, H-1085 Budapest, Hungary

[4] Spectroscopic Research Department, Gedeon Richter Plc., Gyömrői út 19-21, H-1103 Budapest, Hungary

* Correspondence: kupai.jozsef@vbk.bme.hu, kisszekelyi.peter@vbk.bme.hu; Tel.: +36-1-463-2229

Abstract: In this work, anchoring of cinchona derivatives to trifunctional cores (hub approach) was demonstrated to obtain size-enlarged organocatalysts. By modifying the cinchona skeleton in different positions, we prepared four C3-symmetric size-enlarged cinchona derivatives (hub-cinchonas), which were tested as organocatalysts and their catalytic activities were compared with the parent cinchona (hydroquinine) catalyst. We showed that in the hydroxyalkylation reaction of indole, hydroquinine provides good enantioselectivities (up to 73% ee), while the four new size-enlarged derivatives gave significantly lower values (up to 29% ee) in this reaction. Anchoring cinchonas to trifunctional cores was found to facilitate nanofiltration-supported catalyst recovery using PolarClean alternative solvent. The C3-symmetric size-enlarged organocatalysts were completely rejected by all the applied membranes, whereas the separation of hydroquinine was found to be insufficient using organic solvent nanofiltration. Furthermore, the asymmetric catalysis was successfully demonstrated in the case of Michael reaction of 1,3-diketones and *trans*-β-nitrostyrene using **Hub³-cinchona** (up to 96% ee) as a result of the positive effect of the C3-symmetric structure using a bulkier substrate. This means an increased selectivity of the catalyst in comparison to hydroquinine in the latter Michael reaction.

Keywords: cinchona, organocatalysis, C3-symmetry, size-enlargement, nanofiltration, asymmetric reaction

1. Introduction

Over the years, catalysis has been widely explored for more economical and often selective production of high-value products [1]. As preparation of enantiopure organic compounds is of great interest, asymmetric catalysis has developed into a dynamic, rapidly evolving field [2]. Compounds having rotational symmetry gained increased attention in asymmetric synthesis, because they are believed to be able to improve enantioselectivity by decreasing the number of possible transition states during the reaction [3–5]. Due to their beneficial effect on enantioselectivity, C2- and C3-symmetric molecules have been the object of extensive research and, as a result, C3-symmetric compounds have been successfully applied as catalysts, ligands, molecular receptors, supra- and macromolecular constructs, gelators, metal-organic materials (MOMs), etc. [6–11].

Organocatalysts containing three equal catalytic units in a C3-symmetrical fashion have also been studied. Following the application of tripodal phosphinamide ligands in the enantioselective BH_3 reduction of ketones [12–13], Han *et al.* successfully applied tribenzyl- and triphenylphosphine oxide-based proline organocatalysts for aldol reaction [14]. Then, Moorthy *et al.* applied C3-symmetrical organocatalysts by anchoring proline and pyrrolidine to trifunctional trialkylbenzene cores. These C3-symmetric organocatalysts provided the Michael adducts of carbonyl compounds and *trans*-β-nitrostyrene with high stereoselectivities [15]. Beside proline and pyrrolidine, trisimidazoline derivatives were also successfully utilized as catalysts by Fujioka *et al.* in Michael addition reactions, α-amination of β-ketoesters, and bromolactonization of alkenoic acids [16–18]. Later, the application of C3-symmetric trisimidazoline organocatalysts was extended to an enantio- and diastereoselective Betti/aza-Michael sequence as well [19].

Cinchona-based C2- and C3-symmetric compounds have also been widely studied [20]. Jew *et al.* demonstrated the high enantioselectivity of a novel trimeric cinchona alkaloid ammonium salt as phase-transfer catalyst (PTC) in the

catalytic asymmetric alkylation of *N*-(diphenylmethylene)glycine *tert*-butyl ester [21]. Later, the C_3-symmetric cinchona PTC catalyzed asymmetric syntheses of α-amino acids and the highly enantioselective Michael reaction of chalcones and diethyl malonate were performed by Siva *et al.* [22–25]. Csámpai and co-workers examined the *in vitro* antitumor activity of acylated *mono-*, *bis-*, and *tris*-cinchona-based amines [26]. Other than high selectivity, Dong *et al.* also showed the good recyclability of cinchonine squaramide-based C_3-symmetric catalysts in enantioselective Michael addition, in hydroxyalkylation of indoles with alkyl trifluoropyruvate, and in asymmetric chlorolactonization of carboxylic acids [27–30]. These catalysts were easily recovered by precipitation and used from 4 to 6 cycles without significant loss of productivity and selectivity.

Organic solvent nanofiltration (OSN), also called as solvent-resistant nanofiltration (SRNF), is a pressure-driven sustainable separation technology applied in fine chemical and petrochemical purification, which can separate solutes between 50 and 2,000 g mol^{-1} in a wide range of organic solvents [31]. OSN is a predictable and energy-efficient technology compared to other separation techniques such as distillation, chromatography, and extraction [32]. There is an increasing interest in applying OSN for the purification of pharmaceutically relevant compounds [33–36], as well as solvent recovery [37,38]. OSN has also been proposed for the recovery of enlarged metal catalysts [39], and organocatalysts [40]. As an alternative recycling method to precipitation, Livingston *et al.* demonstrated the OSN enabled recovery of C_3-symmetric quinidine-based organocatalysts [41]. The immobilization of cinchonas on trifunctional cores was found to be an effective molecular weight enlargement (MWE) method to facilitate their retention by OSN without destroying the catalytic efficiency of the organocatalysts in Michael addition reactions. Immobilizing organocatalysts on multifunctional cores, the so-called "hub-approach", is an MWE method in which the number of catalytic motifs in the size-enlarged molecule is increased, while the extent of non-functional "spacers" is decreased in comparison to polymer- or dendrimer-based supports. By adjusting the length and type of the linkers between the core (hub) and the catalytic units, the rigidity of the resulting size-enlarged catalyst can be regulated, which has a direct effect on the selectivity experienced in the organocatalytic reactions.

Taking these results into account, we intended to further explore the organocatalytic opportunities of size-enlarged C_3-symmetric cinchona-based organocatalysts. Thus, multiple hub-cinchona structures both with or without H-bond donor capabilities were designed and tested in the hydroxyalkylation of indole and Michael addition reactions, in which the structure-selectivity relationships are also discussed. Finally, the expected superior membrane rejection of the size-enlarged catalysts is presented.

2. Results

During our work, we prepared and explored two types of C_3-symmetric cinchona organocatalysts with varied H-bond donor properties (Figure 1). Compounds belonging to Type A are structurally the simplest as they have no H-bond donor units due to the derivatization of the hydroxyl group (9-OH, see Figure 1c) of the cinchona skeleton during the immobilization process. On the contrary, the mono H-bond donor 9-OH has been reserved in the case of Type B compounds as the cinchona motif was anchored to the hub either through the aromatic quinoline (Williamson ether formation) or through the quinuclidine unit using copper(I) catalyzed azide–alkyne cycloaddition (CuAAC). As a hub, we used 1,3,5-triethynylbenzene, 1,3,5-*tris*(bromomethyl)benzene, or tripropargylamine.
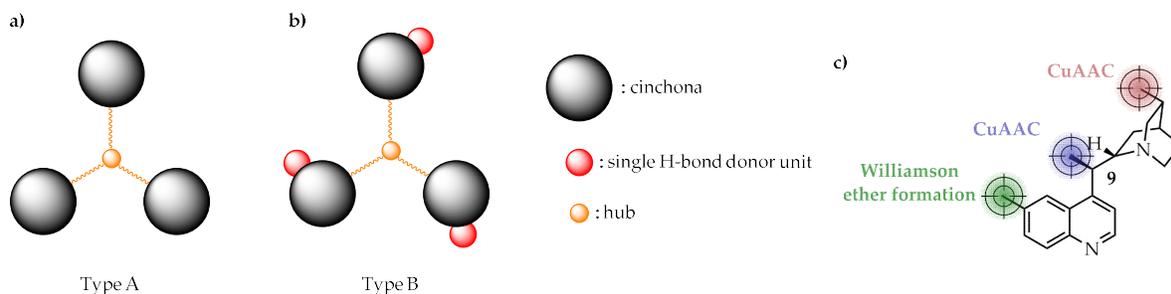

Figure 1. Explored C_3-symmetric hub-cinchona structures containing no (a), or single H-bond donor units (b). Cinchona skeleton was anchored through different positions (c). CuAAC: copper(I) catalyzed azide–alkyne cycloaddition.

2.1. Synthesis of new C_3-symmetric hub-cinchona catalysts

First, we prepared **Hub¹,²-cinchona** (Type A) organocatalysts using a common intermediate (**3**, Scheme 1). Cinchona azide **3** was obtained in two steps: mesylation of hydroquinine (**1**), followed by substitution with azide anion applying NaN₃. Then, azide **3** was reacted with either 1,3,5-triethynylbenzene (**4**), or tripropargylamine (**5**) in CuAAC reaction, which gave **Hub¹-** and **Hub²-cinchona**, respectively, with moderate yields. Having been functionalized at the secondary hydroxyl group of the cinchona moiety, these compounds contain no H-bond donor units. However, other non-covalent interactions can still be formed through the protonated quinuclidine N-atom (ionic) or the aromatic quinoline ring (π–π stacking). Furthermore, the triazole-rings formed by the CuAAC reaction are good electron pair donors, which could interact with metallic species combining the advantageous catalytic qualities of organocatalysts and transition metals to promote new chemical transformations [42, 43].
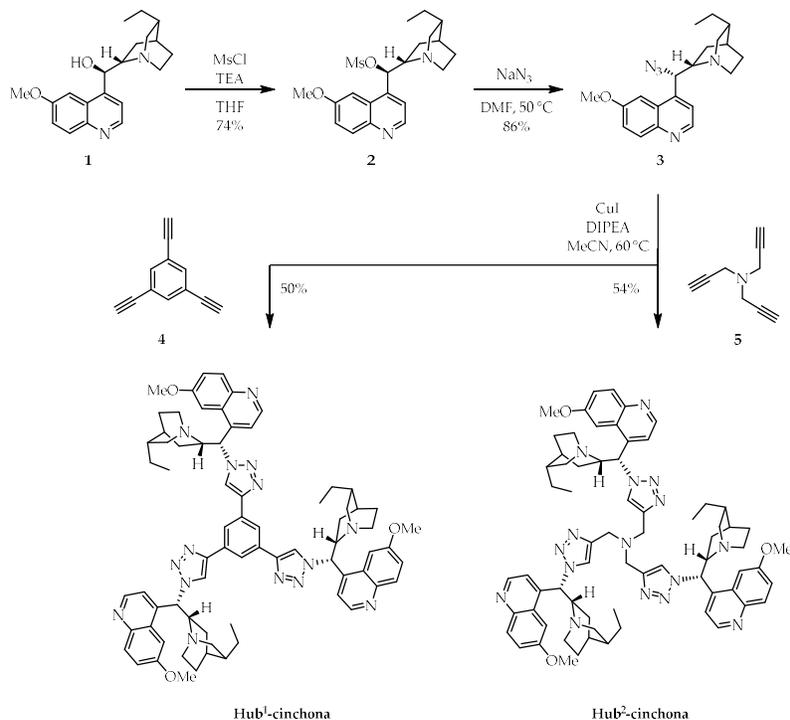

Scheme 1. Syntheses of the size-enlarged C₃-symmetric **Hub¹-** and **Hub²-cinchona** organocatalysts (Type A) by CuAAC using a common cinchona azide intermediate and trifunctional alkynes with different chemical and structural properties. TEA: triethylamine; MsCl: methanesulfonyl chloride; DIPEA: *N,N*-diisopropylethylamine.

Next, cinchona derivatives having mono H-bond donor units (Type B) have been prepared. Hydroquinine (**1**) was demethylated using BBr₃ (1M in DCM) to obtain dihydrocupreine **6** that bears a free phenolic hydroxyl group (Scheme 2). Then, using Cs₂CO₃, as a base, the phenolate of **6** was formed, which could react with 1,3,5-*tris*(bromomethyl)benzene (**7**) in a Williamson etherification reaction to give the size-enlarged organocatalyst **Hub³-cinchona** in good yield. Consequently, we connected the cinchona motif to the core through a stable ether bond, and the H-bond donor hydroxyl group remained intact.
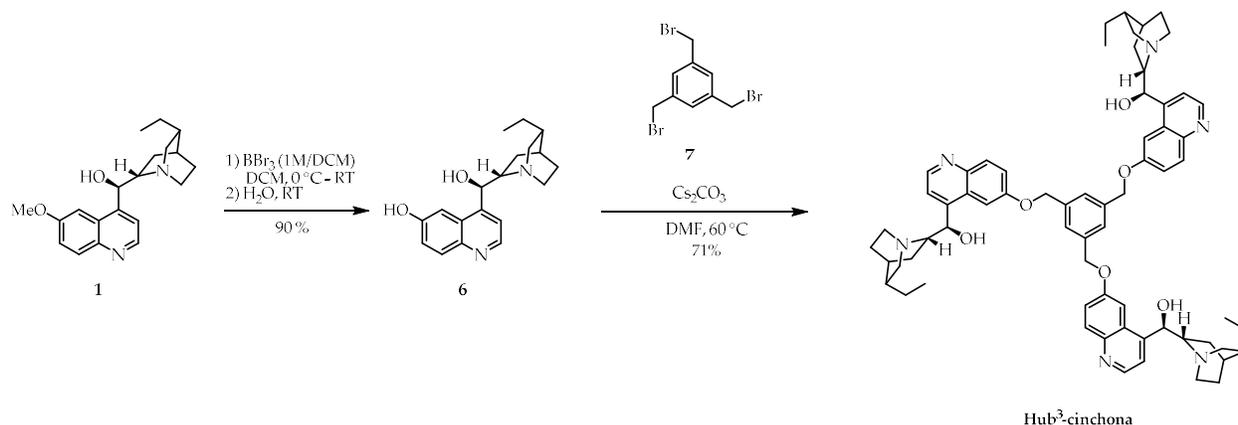
Scheme 2. Synthesis of the size-enlarged C₃-symmetric **Hub³-cinchona** organocatalyst by Williamson ether formation.

Organocatalyst **Hub⁴-cinchona** was prepared in a convergent synthesis (Scheme 3) utilizing an alternative anchoring method. We converted the commercially available quinine (**8**) into didehydroquinine (**9**) using a Br₂ addition–HBr elimination reaction. In a separate reaction, we reacted 1,3,5-*tris*(bromomethyl)benzene (**7**) with NaN₃ in a mixture of water:acetone (1/100) to give the triazido-derivative **10**. Finally, alkyne **9** and triazide **10** were subjected to CuAAC reaction, which gave organocatalyst **Hub⁴-cinchona** with moderate yield.
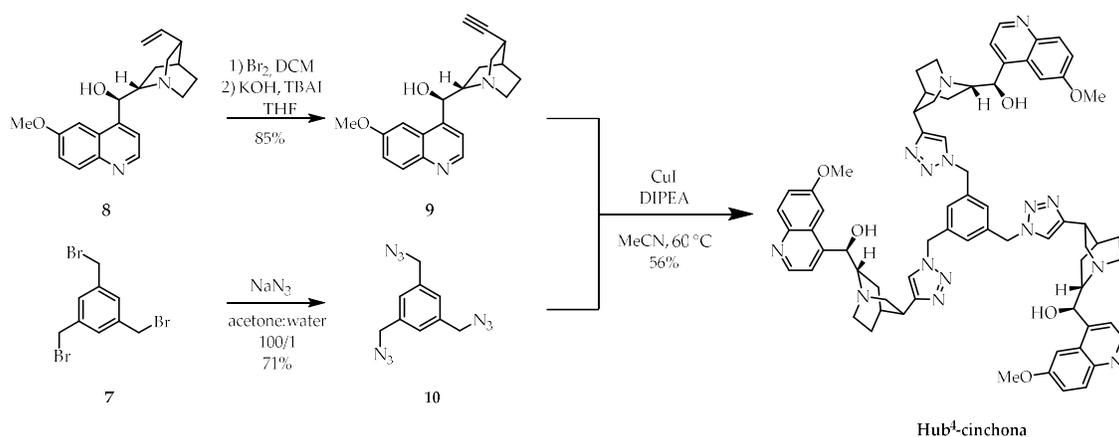
Scheme 3. Convergent synthesis of size-enlarged C₃-symmetric **Hub⁴-cinchona** organocatalyst by CuAAC using a triazide core unit. TBAI: tetra-*n*-butylammonium iodide; DIPEA: *N,N*-diisopropylethylamine.

2.2. Application of hub-cinchona catalysts in hydroxyalkylation of indole and Michael addition reactions

We started our organocatalytic reactions with the hydroxyalkylation of indole. First, the optimal solvent and reaction time were chosen using 5 mol% hydroquinine (**1**), the parent catalytic unit of the hub-cinchona derivatives. As solvents, 11 conventional and alternative ones were used (Table 1). In general, ether-type solvents showed better enantioselectivities in this reaction, while the protic ethanol gave practically racemic product. Regarding conversion, in toluene and ethanol we achieved almost complete transformation, but the other solvents gave also good results (>67%). For the subsequent experiments, cyclopentyl methyl ether (CPME) was chosen, because this solvent provided the best enantioselectivity (73% ee) and the conversion was still good after 24 h stirring at 0 °C (82%). Based on the ¹⁹F NMR spectra, the conversion did not change significantly when the reaction time was reduced to 1 h.

Table 1. Hydroquinine (**1**) catalyzed indole hydroxyalkylation reaction in different solvents.[1]
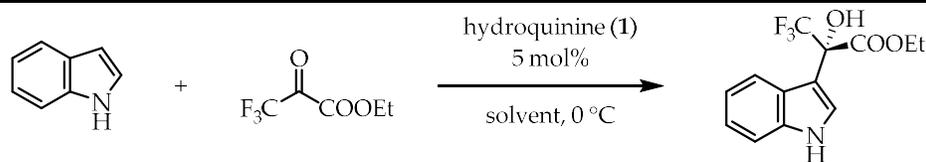
Solvent	Reaction time (h)	Enantiomeric excess (13, %)[1]	Conversion (13, %)[2]
CPME	24	73	82
2-MeTHF	24	69	70
MTBE	24	67	88
DME	24	64	81
toluene	24	61	98
EtOAc	24	59	70
PolarClean	24	52	67
DMC	24	52	92
DCM	24	48	99
MeCN	24	36	82
EtOH	24	2	98
CPME	4	73	87
CPME	2	72	85
CPME	1	72	87

[1] Reaction conditions: indole (1 eq), ethyl trifluoropyruvate (1 eq), 0.015 mmol catalyst mL^{-1} solvent; [2] Determined by chiral HPLC; [2] Determined by ^{19}F NMR; CPME: cyclopentyl methyl ether; 2-MeTHF: 2-methyltetrahydrofuran; MTBE: *tert*-butyl methyl ether; DME: dimethoxyethane; PolarClean: methyl 5-(dimethylamino)-2-methyl-5-oxopentanoate.

With the best solvent and reaction time in hand, we used our newly prepared hub-cinchona organocatalysts in the hydroxyalkylation reaction (Table 2). While the conversion was only slightly lower (~10% difference), the size-enlarged catalysts showed significantly lower enantioselectivities in comparison to hydroquinine (**1**). The highest enantiomeric excess was achieved with **Hub⁴-cinchona** (29% ee), while **Hub²-cinchona** practically provided the hydroxyalkylated product as a racemic mixture (2% ee). Due to the tripropargylamine hub, the latter catalyst (**Hub²-cinchona**) contains a competitive basic unit with the quinuclidine N-atom, which can explain the lack of enantioselectivity. Comparing the structural features of the other catalysts, we can conclude that **Hub¹-** and **Hub⁴-cinchonas** have more rigid structures, which can be attributed to the triazole rings serving also as spacers between the hub and the catalytically active motifs. Therefore, the cinchona units in these cases are more separated from each other. Still, the formation of non-covalent interactions between the individual catalytic motifs within the hub-cinchonas can explain, in general, the significantly lower enantioselectivity and why **Hub¹,⁴-cinchonas** gave better results than the structurally more flexible **Hub³-cinchona**.

Table 2. Hydroquinine (**1**) and **Hub¹⁻⁴-cinchonas** catalyzed indole hydroxyalkylation reaction.[1]

Catalyst	Enantiomeric excess (13, %)[2]	Conversion (13, %)[3]
hydroquinine (**1**)	72	87
Hub¹-cinchona	26	78
Hub²-cinchona	2	77
Hub³-cinchona	18	69
Hub⁴-cinchona	29	72
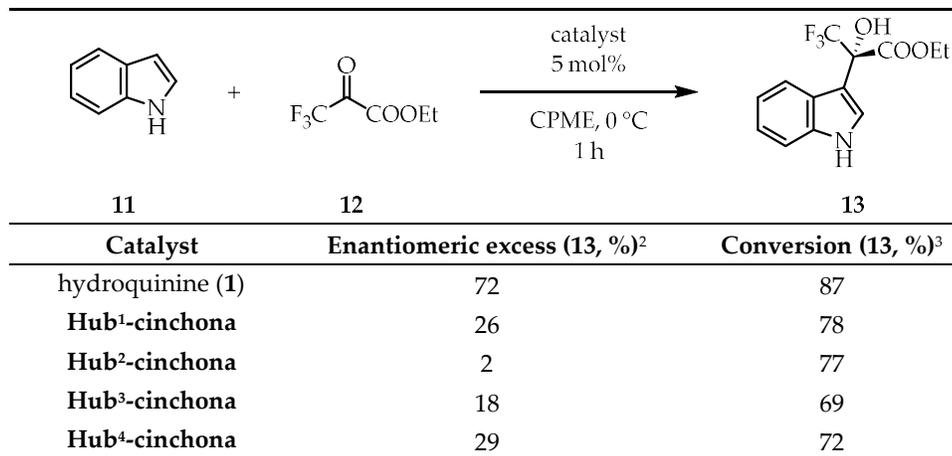
[1] Reaction conditions: indole (1 eq), ethyl trifluoropyruvate (1 eq), 0.016 mmol catalyst mL⁻¹ solvent; [2] Determined by chiral HPLC; [3] Determined by ¹⁹F NMR.

As the solvent can significantly alter the formation of non-covalent interactions, we performed the complete solvent screen with **Hub³-cinchona** (Table 3). While no higher enantioselectivity was achieved, the previously observed trend was still recognizable: ether-type solvents gave good results, but the protic ethanol promoted the formation of the racemic product. Interestingly, in some cases (toluene, DCM, and MeCN) the other antipode of **13** was found to be present in excess.

Table 3. Hub³-cinchona catalyzed indole hydroxyalkylation reaction in different solvents.[1]

Solvent	Enantiomeric excess (13, %)[2]	Solvent	Enantiomeric excess (13, %)[2]
CPME	18	PolarClean	10
2-MeTHF	12	DMC	4
MTBE	12	DCM	-11
DME	13	MeCN	-13
toluene	-4	EtOH	0
EtOAc	2		
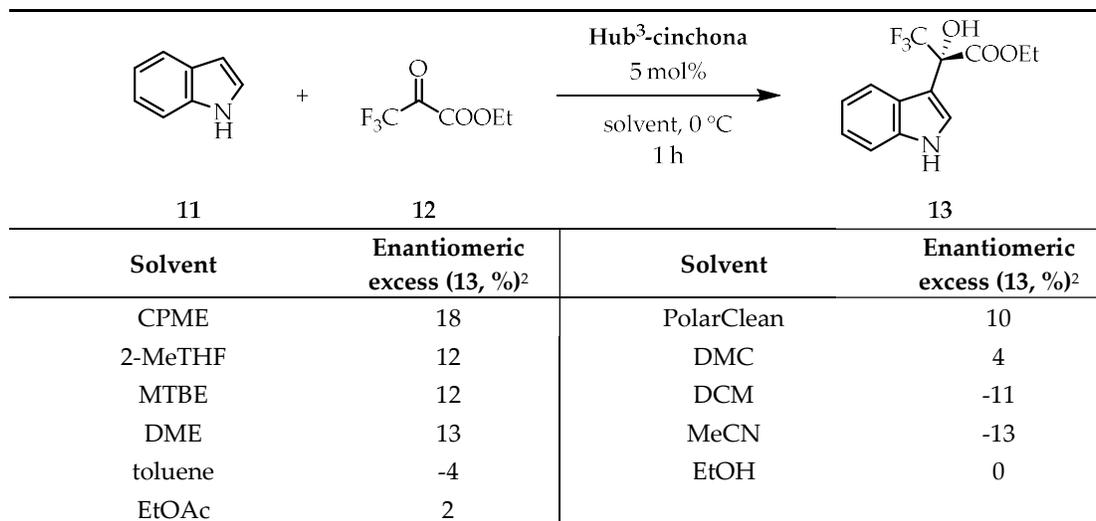
[1] Reaction conditions: indole (1 eq), ethyl trifluoropyruvate (1 eq), 0.0165 mmol catalyst mL⁻¹ solvent; [2] Determined by chiral HPLC; CPME: cyclopentyl methyl ether; 2-MeTHF: 2-methyltetrahydrofuran; MTBE: *tert*-butyl methyl ether; DME: dimethoxyethane; PolarClean: methyl 5-(dimethylamino)-2-methyl-5-oxopentanoate.

Additionally, the catalytic efficiencies of the size-enlarged hub-cinchonas and hydroquinine (**1**) were also compared in the Michael addition reaction of pentane-2,4-dione (**14**) and *trans*-β-nitrostyrene (**15**). The applied reaction conditions were chosen based on our previous work [44]. Based on the measured enantioselectivities (Table 4), hydroquinine (**1**) is not a suitable catalyst for this reaction (-14% ee). While organocatalysts **Hub¹,²,⁴-cinchonas** gave nearly racemic mixtures, **Hub³-cinchona** showed two times higher enantioselectivity than catalyst **1** (32% ee *vs.* -14% ee) with a preference to the mirror image stereoisomer.

Table 4. Hydroquinine (**1**) and hub-cinchona catalyzed Michael addition reaction of pentane-2,4-dione and *trans*-β-nitrostyrene.[1]
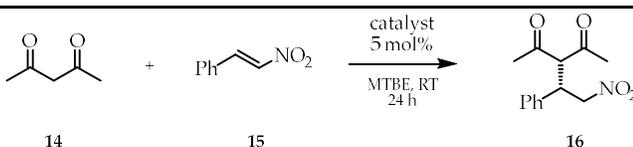
Catalyst	Enantiomeric excess (16, %)[2]	Yield (16, %)[3]
hydroquinine (**1**)	-14	82
Hub¹-cinchona	3	10
Hub²-cinchona	1	24
Hub³-cinchona	32	82
Hub⁴-cinchona	1	78

[1] Reaction conditions: diketone (2.5 eq), nitrostyrene (1 eq), 0.015 mmol catalyst mL⁻¹ solvent; [2] Determined by chiral HPLC; [3] Yield of isolated product purified by preparative TLC.

Considering that these two catalysts (**1** and **Hub³-cinchona**) are structurally very similar in regard to catalytical motif(s), the higher selectivity clearly suggests that the C_3-symmetric structural feature of the size-enlarged **Hub³-cinchona** has a positive effect on the enantioselectivity. This advantageous outcome can be attributed either to the formation of a sterically more hindered space during the transition state or to an alternative catalyst–substrate interaction layout including two or more cinchona motifs. To see how a bulkier substrate affects the enantioselectivity of this reaction, the Michael addition of 1,3-diphenylpropane-1,3-dione (**17**, Scheme 4) and *trans*-β-nitrostyrene (**15**) was also performed using **Hub³-cinchona**. Although only 1 mol% of catalyst was used, the enantioselectivity increased significantly regardless of the solvent (2 mL), like DCM (53% ee), EtOAc (64% ee), MeCN (71% ee), or toluene (80% ee). The best result was achieved by using MTBE. In this case the selectivity reached 93% ee, and the yield was 69% after purification by preparative TLC. In comparison, the reaction catalyzed by hydroquinine (**1**) gave only 6% ee with 84% preparative yield.

To conclude, the Michael addition reaction showed increased selectivity for the size-enlarged **Hub³-cinchona** catalysts compared to its cinchona unit (hydroquinine, **1**), which indicates the positive effect of the C_3-symmetric structure. Furthermore, Michael adduct prepared form bulkier substrate was obtained with excellent enantioselectivities (up to 96% ee) when **Hub³-cinchona** was applied.
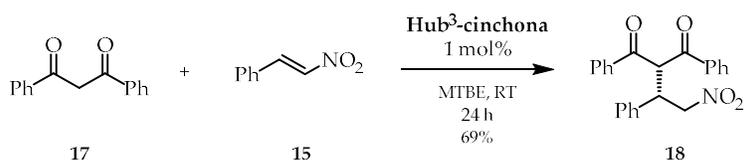
Scheme 4. Michael addition of 1,3-diphenylpropane-1,3-dione (**17**) and *trans*-β-nitrostyrene (**15**) catalyzed by **Hub³-cinchona** organocatalyst.

2.3. Membrane rejection of hub-cinchona organocatalysts

Given the bulky nature of the size-enlarged catalysts, they are fully retained on all the tested membranes with rejection values of 100% (Figure 2a). It is important to achieve 100% rejection to avoid the loss of any valuable catalyst during the recovery process. The rejections of indole (**11**) and hydroxyalkylated product **13** vary between 5% and 55% depending on both the membrane and the molecular weight. For efficient catalyst recovery, the rejection gap between the catalyst and the other solutes needs to be as large as possible. Consequently, one can conclude that the best membrane for the bub-cinchona organocatalysts recovery is DM900. This membrane exhibited substrate solute rejections below 30%, while still maintaining complete retention of the catalysts. Moreover, DM900 is the most open membrane with the highest flux of 6.7±0.24 L m⁻² h⁻¹ (Figure 2b). It is important to maximize the flux in order to achieve an efficient catalyst recovery process. Comparing the membrane rejections of the hub-cinchonas with hydroquinine (**1**),

the advantage of molecular size-enlargement can be clearly seen. Due to the similar rejection values of hydroquinine (**1**) and product **13**, membrane recovery of **1** from the reaction mixture would be inadequate.
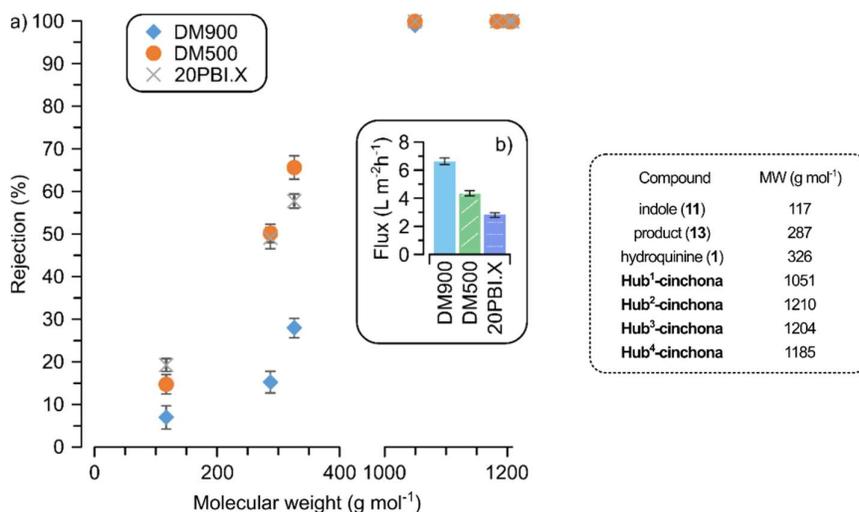

Figure 2. Rejection (a) and flux (b) values for the three screened solvent-resistant membranes in PolarClean green solvent at 10 bar in crossflow mode.

3. Materials and Methods

3.1. General Information

Starting materials were purchased from commercially available sources (Sigma-Aldrich, Merck, and Alfa Aesar). Infrared spectra were recorded on a Bruker Alpha-T FT-IR spectrometer (Bruker, Ettlingen, Germany). Optical rotations were measured on a Perkin-Elmer 241 polarimeter (Perkin-Elmer, Waltham, MA, USA) that was calibrated by measuring the optical rotations of both enantiomers of menthol. Silica gel 60 F$_{254}$ (Merck) and aluminium oxide 60 F$_{254}$ neutral type E (Merck) plates were used for TLC. Aluminium oxide (neutral, activated, Brockman I) and silica gel 60 (70–230 mesh, Merck) were used for column chromatography. Ratios of solvents for the eluents are given in volumes (mL mL^{-1}). Melting points were taken on a Boetius micro-melting point apparatus (VEB Dresden Analytik, Dresden, Germany) and they were uncorrected. *N*,*N*-Dimethylacetamide (DMAc) solution of polybenzimidazole (PBI, 26 wt%) was purchased from PBI Performance Products (USA). The previously reported 20PBI.X membrane was obtained based on Schaepertoens *et al.* [45]. PBI was selected as it is an emerging polymer for OSN [46,47]. DuraMem solvent-resistant membranes (DM500 and DM900) can be obtained from Evonik (Germany). PolarClean solvent is produced by Solvay (Italy). NMR spectra were recorded either on a Bruker DRX-500 Avance spectrometer (at 500 MHz for ^{1}H, at 125 MHz for ^{13}C, and at 376 MHz for ^{19}F spectra) or on a Bruker 300 Avance spectrometer (at 300 MHz for ^{1}H, at 75 MHz for ^{13}C, and at 222.5 MHz for ^{19}F spectra) or on a Bruker Avance III HD (at 600 MHz for ^{1}H and at 150 MHz for ^{13}C spectra). HPLC-MS was performed on an HPLC system using Agilent Technologies 1200 Series - Agilent Technologies 6130 Quadrupole; column: Phenomenex Kinetex C18 100A (2.6 µm, 50 × 3.00 mm); A eluent: water (1% HCOONH$_4$); B eluent: MeCN (8% water, 1% HCOONH$_4$); gradient: 20% – 100%. In case of indole hydroxyalkylation, HPLC-MS was performed using a Shimadzu LCMS-2020 (Shimadzu Corp., Kyoto, Japan) device, equipped with a Reprospher (Altmann Analytik Corp., München, Germany) 100 C18 (5 µm, 100 × 3 mm) column and a positive/negative double ion source (DUIS±) with a quadrupole MS analyzer in a range of 50–1000 m/z. The samples were eluted with gradient elution, using eluent A (0.1% formic acid in water) and eluent B (0.1% formic acid in MeCN). The flow rate was set to 1.5 mL min^{-1}. The initial condition was 5% eluent B, followed by a linear gradient to 100% eluent B by 1.5 min; from 1.5 to 4.0 min, 100% eluent B was retained; and from 4 to 4.5 min, it went back by a linear gradient to 5% eluent B, which was retained from 4.5 to 5 min. The column temperature was kept at room temperature, and the injection volume was 1–10 µL. The purity of the compounds was assessed by HPLC with UV detection at 215 and 254 nm. High resolution mass measurements were performed on a Thermo Exactive plus EMR Orbitrap mass spectrometer, which was used with a Thermo Ultimate 3000

UHPLC with 100% methanol as the mobile phase. The enantiomeric ratios of the samples were determined by chiral high-performance liquid chromatography (HPLC) measurements using either reversed-phase mode (Thermo Finnigan Surveyor LC System, Thermo Fisher Scientific, Waltham, MA, USA) or normal phase mode (PerkinElmer Series 200 LC System, PerkinElmer, Inc, Shelton, CT, USA), and the exact conditions are indicated in the correspondent asymmetric reaction in the Experimental section.

3.2. Preparation of Compounds

*(1R)-(–)-((2S,4S,5R)-5-Ethylquinuclidin-2-yl)(6-methoxyquinolin-4-yl)methyl methanesulfonate (**2**):*
      This compound was prepared based on the description in the literature [48]. A solution of hydroquinine (**1**, 3.00 g, 9.19 mmol, 1.0 eq) in dry THF (55 mL) was stirred under Ar at 0 °C. To this solution was added triethylamine (6.2 mL, 44.1 mmol, 4.8 eq), then methanesulfonyl chloride (2.9 mL, 36.8 mmol, 4.0 eq) was added dropwise. Next, the reaction mixture was allowed to warm up to room temperature, and it was stirred for 4 h. The solvent was evaporated under reduced pressure. The residue was dissolved in a mixture of DCM (50 mL) and sat. aqueous solution of $NaHCO_3$ (50 mL). The aqueous phase was extracted with DCM (2 × 50 mL). The combined organic phase was dried over anhydrous $MgSO_4$, filtered, and the solvent was removed under reduced pressure. The crude product was purified by column chromatography (silica gel, MeOH/toluene 1:6) to obtain hydroquinine mesylate (**2**, 2.20 g, 73%) as a yellow solid.
      R_f: 0.37 (silica gel, MeOH/toluene 1:4); Mp: 102.9–104.3 °C (lit Mp: 105–108 °C) [47]; MS-ESI+ (m/z): [M + H]+ calcd for $C_{21}H_{29}N_2O_4S$: 405.2, found: 405.0. Spectroscopic data are fully consistent with those reported in the literature [49].

*(2S,4S,5R)-(+)-2-((S)-Azido(6-methoxyquinolin-4-yl)methyl)-5-ethylquinuclidine (**3**):*
      Compound **3** was prepared based on the description in the literature [48]. A solution of mesylate **2** (2.00 g, 4.94 mmol, 1.0 eq) in dry DMF (55 mL) was stirred under Ar atmosphere at room temperature. To this solution NaN_3 was added (1.45 g, 22.3 mmol, 4.5 eq). Next, the reaction mixture was warmed up to 45 °C and it was stirred at this temperature until the reaction was completed. The solvent was evaporated under reduced pressure, then water was added to the residue, and this aqueous mixture was extracted with Et_2O (3 × 15 mL). The combined organic phase was evaporated to obtain azido-hydroquinine as a yellow oil (**3**, 1.44 g, 83%) and used without further purification.
      R_f: 0.20 (silica gel, DCM/MeOH 10:1); MS-ESI+ (m/z): [M + H]+ calcd for $C_{20}H_{26}N_5O_4$: 352.2, found: 352.1. Spectroscopic data are fully consistent with those reported in the literature [50].

*Dihydrocupreine (**6**):*
      Hydroquinine (**1**, 1.00 g, 3.06 mmol, 1.0 eq) was dissolved in DCM (90 mL) under Ar atmosphere, then this solution was cooled to 0 °C. Next, BBr_3 (1 M DCM solution, 26.0 mL, 26.0 mmol, 8.5 eq) was added dropwise. Next, the reaction mixture was left to slowly warm up to room temperature, and it was stirred overnight. After complete consumption of the starting material (TLC, silica gel, DCM/MeOH/NH_4OH 5:1:0.01), a solution of 10% NaOH (aq., 40 mL) was added to the mixture. Following the separation of the two phases, the aqueous phase was washed with DCM (3 × 50 mL). Next, cc. HCl (aq.) was added to neutralize the aqueous phase, followed by extraction with DCM (3 × 50 mL). The combined organic phase was dried over anhydrous $MgSO_4$, filtered, and the solvent was evaporated under reduced pressure to yield **6** (860 mg, 90%) as a brown solid.
      R_f: 0.12 (silica gel; MeOH/toluene 1:4); $[\alpha]_D^{25}$: -180.9° (c 1.00, $CHCl_3$); Mp. 224.4–225.9 °C (lit. Mp. 230 °C, [51]). Spectroscopic data are fully consistent with those reported in the literature [52].

*(R)-[(2S,4S,5S)-5-Ethynylquinuclidine-2-yl)(6-methoxyquinoline-4-yl]methanol (**9**)*
      To a solution of quinine (**8**, 5.00 g, 15.4 mmol, 1.0 eq) in DCM (150 mL) was added a mixture of Br_2 (1.70 mL, 30.9 mmol, 2.0 eq) and DCM (7 mL) at 0 °C. The reaction mixture was stirred at 0 °C for 1 h while a yellow solid precipitated. After stirring the reaction mixture for an additional hour at room temperature, hexane (300 mL) was added, stirred for 10 min, and filtered. The filtrate was washed with hexane and dried under infrared lamp for 1 h. The yellow solid was dissolved in THF (150 mL), and TBAI (550 mg, 1.71 mmol, 0.1 eq) was added to this solution. Then, finely powdered KOH (5.00 g, 89.1 mmol, 5.8 eq) was added to the mixture, and stirred at 45 °C for 1 h when an additional batch of KOH (5.00 g, 89.1 mmol, 5.8 eq) was added to it. The reaction mixture was stirred for 12 h at room temperature. After complete consumption of the starting materials (TLC, silica gel, MeOH/DCM/TEA 1:10:0.2), the mixture was filtered, dried over anhydrous $MgSO_4$, and the solvent was removed under reduced pressure. The crude product was purified by dry column vacuum chromatography (silica gel, EtOAc/NH_4OH 20:1, EtOAc/NH_4OH/MeOH 95:5–45:55) to yield **9** (4.25 g, 85%) as a brown solid.

R_f: 0.50 (silica gel, MeOH/DCM/TEA 1:10:0.2). Mp. 167–170 °C; Spectroscopic data are fully consistent with those reported in the literature [53].

*1,3,5-Tris(azidomethyl)benzene (**10**)*

Tris(bromomethyl)benzene (**7**, 500 mg, 1.40 mmol, 1.0 eq) was dissolved in a mixture of acetone/H_2O 1:0.01 (10 mL), then NaN_3 (550 mg, 8.50 mmol, 6.1 eq) was added, and the resulting mixture was stirred at room temperature for 1 day. After consumption of the starting material (TLC, silica gel, EtOAc/hexane 1:2), the mixture was concentrated, and to the remaining aqueous mixture EtOAc (15 mL) and water (15 mL) were added. The separated organic phase was washed with water (2 × 15 mL), dried over anhydrous $MgSO_4$, filtered, and the solvent was removed under reduced pressure to yield **10** (244 mg, 71%) as an oil. This product was used without further purification.

R_f: 0.65 (silica gel, EtOAc/hexane 1:2). Spectroscopic data are fully consistent with those reported in the literature [54]. Although the *tris*(azidomethyl)benzene is reported to be relatively insensitive to heat and shock, special care was taken during its synthesis and application to avoid accidents [54,55].

Hub¹-cinchona

To a mixture of cinchona azide (**3**, 700 mg, 2.00 mmol, 6.0 eq), 1,3,5-triethynylbenzene (**4**, 50 mg, 0.33 mmol, 1.0 eq) and DIPEA (1.22 mL, 7.00 mmol, 21.0 eq) a suspension of CuI (38 mg, 0.20 mmol, 0.6 eq) in MeCN (1 mL) was added. The mixture was stirred at 60 °C for 2 days. After complete consumption of the starting material (TLC, silica gel, MeOH/DCM/NH_4OH 1:10:0.01), the solvent was evaporated under reduced pressure, and the crude product was purified by column chromatography (silica gel, MeOH/DCM/NH_4OH 1:20:0.01–1:5:0.01 to yield **Hub¹-cinchona** (200 mg, 50%) as light-yellow solid.

R_f: 0.40 (silica gel, MeOH/DCM/NH_4OH 1:10:0.01); Mp. 195 °C; ¹H NMR (600 MHz, DMSO-d_6): δ 0.85 (m, 12H), 1.40 (m, 9H), 1.53 (overlapping, 3H), 1.63 (s, 6H), 1.73 (br, 3H), 2.41 (d, J = 12.6 Hz, 3H), 2.96 (m, 3H), 3.43 (overlapping, 3H), 3.99 (s, 9H), 4.09 (overlapping, 3H), 6.64 (m, 3H), 7.46 (m, 3H), 7.85 (br, 3H), 7.88 (d, J = 6.0 Hz, 3H), 7.98 (d, J = 6.0 Hz, 3H), 8.11 (m, 3H), 8.86 (m, 6H); HPLC-MS-ESI⁺ (m/z): [M + H]⁺ calcd for $C_{72}H_{81}N_{15}O_3$: 1203.66, found: 1204.44.

Hub²-cinchona

To a mixture of cinchona azide (**3**, 803 mg, 2.29 mmol, 6.0 eq), tripropargylamine (**5**, 50 mg, 0.38 mmol, 1.0 eq) and DIPEA (1.39 mL, 8.00 mmol, 21.0 eq) was added a suspension of CuI (44 mg, 0.23 mmol, 0.6 eq) in MeCN (1 mL). The mixture was stirred at 60 °C for 2 days. After complete consumption of the starting material (TLC, silica gel, MeOH/DCM/NH_4OH 1:10:0.01), the solvent was evaporated under reduced pressure, and the crude product was purified by column chromatography (silica gel, MeOH/DCM/NH_4OH 1:20:0.01–1:5:0.01 to yield **Hub²-cinchona** (243 mg, 54%) as light-yellow solid.

R_f: 0.40 (silica gel, MeOH/DCM/NH_4OH 1:10:0.01); Mp. 162 °C; ¹H NMR (600 MHz, DMSO-d_6): δ 0.73 (br, 3H), 0.82 (m, 9H), 1.35 (overlapping, 9H), 1.60 (overlapping, 9H), 2.46 (br, 3H), 2.90 (br, 3H), 3.42 (overlapping, 9H), 3.89 (s, 9H), 3.98 (br, 3H), 6.52 (br, 3H), 7.43 (m, 3H), 7.74 (br, 3H), 7.82 (m, 3H), 7.96 (d, J = 9.0 Hz, 3H), 8.16 (overlapping, 3H), 8.78 (m, 3H). HPLC-MS-ESI⁺ (m/z): [M + H]⁺ calcd for $C_{69}H_{84}N_{16}O_3$: 1184.69, measured: 1185.54; HRMS-ESI⁺ (m/z): [M + H]⁺ calcd for $C_{69}H_{84}N_{16}O_3$: 1185.6985, found: 1185.6951.

Hub³-cinchona

To a solution of dihydrocupreine (**6**, 500 mg, 1.60 mmol, 6.0 eq) in dry DMF (50 ml) Cs_2CO_3 (772 mg, 2.39 mmol, 9.0 eq) was added, and the resulting mixture was stirred at 60 °C for 1 h. Next, 1,3,5-*tris*(bromomethyl)benzene (**7**, 95 mg, 0.27 mmol, 1.0 eq) was added to the mixture, and stirred for 3 h. Then, the solvent was evaporated, and the residue was taken up in a mixture of EtOAc (50 mL) and H_2O (50 mL). The forming brown precipitate was filtered and washed with EtOAc (3 × 20 mL) to yield **Hub³-cinchona** (398 mg, 71 %) as a brown solid.

R_f: 0.41 (aluminium oxide, MeOH/DCM/NH_4OH 10:1:0.01); Mp. 166–175 °C; IR (film) v_{max}: 3267, 2929, 2871, 1618, 1590, 1507, 1457, 1378, 1359, 1325, 1238, 1217, 1131, 1115, 1085, 1052, 1024, 1004, 937, 880, 857, 820, 758, 693, 642, 620, 609, 568, 549, 530, 467, 435, 417, 401 cm⁻¹; ¹H NMR (500 MHz, DMSO-d_6): δ 0.71–0.78 (t, J =7.0 Hz, 9H), 1.21–1.23 (m, 3H), 1.24–1.28 (m, 6H), 2.07–2.15 (m, 3H), 2.26–2.30 (m, 6H), 2.65–2.69 (m, 6H), 2.70–2.73 (m, 6H), 2.77–2.79 (m, 6H), 2.98–3.01 (m, 3H), 5.32 (s, 6H), 6.48 (br s, 3H), 7.45 (s, 3H), 7.48–7.50 (d, J =5.0 Hz, 3H), 7.63–7.68 (s, 6H), 7.84–7.87 (d, J =9.0 Hz, 3H), 7.92–7.95 (d, J = 4.0 Hz, 3H); ¹³C NMR (125 MHz, DMSO-d_6): δ 11.9, 20.6, 25.1, 27.2, 28.2, 37.1, 41.8, 60.6, 69.5, 71.0, 79.2, 103.9, 121.2, 122.0, 126.1, 127.1, 131.2, 137.5, 141.6, 144.0, 146.0, 158.6; HPLC-MS-ESI⁺ (m/z): [M + H]⁺ calcd for $C_{66}H_{78}N_6O_6$: 1050.60, found: 1051.80.

Hub⁴-cinchona

To a mixture of triazide (**10**, 110 mg, 0.45 mmol, 1.0 eq), cinchona derivative **9** (875 mg, 2.71 mmol, 6.0 eq) and DIPEA (1.66 mL, 9.49 mmol, 21.0 eq) a suspension of CuI (51.7 mg, 0.27 mmol, 0.6 eq) in MeCN (3 mL) was added. The mixture was stirred at 60 °C for 2 days. After complete consumption of the starting material (TLC, silica gel, MeOH/DCM/NH$_4$OH 1:5:0.01, or DCM/hexane 1:2), the solvent was evaporated under reduced pressure, and the crude product was purified by column chromatography (aluminium oxide, MeOH/DCM/NH$_4$OH 1:20:0.01–1:5:0.01 to yield **Hub⁴-cinchona** (306 mg, 56%) as a light-brown solid.

R$_f$: 0.49 (aluminium oxide, MeOH/DCM/NH$_4$OH 1:20:0.01); Mp. 179–180 °C; ¹H NMR (600 MHz, DMSO-d$_6$): δ 1.53 (m, 3H), 1.57 (m, 6H), 1.71 (m, 3H), 1.98 (m, 3H), 2.52 (m, 3H), 2.87 (m, 3H), 2.96 (m, 3H), 3.02 (m, 3H), 3.20 (m, 3H), 3.21 (m, 3H), 3.88 (s, 9H), 5.23 (m, 3H), 5.46 (s, 6H), 5.62 (d, *J* =5.1 Hz, 3H), 7.08 (s, 3H), 7.38 (dd, *J* =2.8; 9.2 Hz, 3H), 7.48 (d, *J* =4.5 Hz, 3H), 7.51 (d, *J* =4.5 Hz, 3H), 7.92 (d, *J* =9.2 Hz, 3H), 7.93 (s, 3H), 8.86 (d, *J* =4.5 Hz, 3H); ¹³C NMR (600 MHz, DMSO-d$_6$): δ 24.5, 27.5, 27.7, 32.8, 42.1, 52.4, 55.5, 55.6, 60.6, 71.1, 102.7, 119.4, 121.2, 122.2, 126.9, 127.4, 131.3, 137.6, 144.1, 147.7, 149.5; 150.7; 156.9; HPLC-MS-ESI$^+$ (m/z): [M + H]$^+$ calcd for C$_{69}$H$_{75}$N$_{15}$O$_6$: 1209.60, measured: 1210.40; HRMS-ESI$^+$ (m/z): [M + H]$^+$ calcd for C$_{69}$H$_{75}$N$_{15}$O$_6$: 1210.60975, found: 1210.61203.

General procedure for the indole hydroxyalkylation reaction: ethyl (S)-(+)-3,3,3-trifluoro-2-hydroxy-2-(1H-indol-3-yl)propanoate (13)

To a solution of indole (**11**, 1.0 eq) in the given solvent was added the organocatalyst (5 mol%) and the resulting reaction mixture was stirred for 1 h at 0 °C. Next, ethyl trifluoropyruvate (**12**, 1.0 eq) was added to it, and stirred further at 0 °C. After the corresponding reaction time (see Table 1–3) the volatile components were removed under reduced pressure. The crude product was purified by preparative thin-layer chromatography (R$_f$: 0.45, silica gel, DCM) to give product **13** as a solid.

R$_f$: 0.45 (silica gel, DCM); $[\alpha]_D^{25}$: +9.1 (CHCl$_3$, *c* 1.00, 87% ee, *S* config.) (lit. $[\alpha]_D^{25}$: +11.3, CHCl$_3$, *c* 1.01, 74% ee, *S* config. [56]); Colorless crystals. Mp. 71– 72°C (lit. Mp: 70.5–71.8 °C, [57]); MS-ESI- (m/z): [M – H$^+$]$^-$ 286; The conversion was determined by ¹⁹F NMR. Enantiomeric excess was determined by reversed phase HPLC analysis using Phenomenex Lux Cellulose-1 (5 µm, 250 x 4.6 mm) column, eluent water (0.1% NH$_4$OAc)/MeCN = 40/60, 0.8 mL min^{-1}, UV detector 222 nm. Retention time for (*R*)-**13** and (*S*)-**13** are 6.5 min and 7.2 min, respectively. Spectroscopic data are fully consistent with those reported in the literature [57].

General procedure for the Michael addition reaction:

To a solution of 1,3-dioxo compound (**14** or **17**, 2.5 eq) and *trans*-β-nitrostyrene (**15**, 1.0 eq) in the given solvent catalyst (5 or 1 mol%) was added. The resulting mixture was stirred at room temperature for 24 h. Then, the volatile components were removed under reduced pressure. The crude product was purified by thin-layer chromatography (hexane/EtOAc, 2:1 for compound **16**, and 4:1 for compound **18**) to give the Michael adduct as a solid.

(*S*)-(+)-3-(2-Nitro-1-phenylethyl)pentane-2,4-dione (**16**): R$_f$: 0.13 (silica gel, hexane/EtOAc, 4:1); $[\alpha]^{25}$: +195.2 (CHCl$_3$, *c* 1.00, 99.1% ee, *S* config.) (lit. $[\alpha]_D^{25}$: +196.7, CHCl$_3$, *c* 1.01, 88% ee, *S* config. [58]); White crystals. Mp. 125–128 °C (lit. Mp: 124–126 °C, [58]); MS-ESI+ (m/z): [M + NH$_4$]$^+$ 267.1; Enantiomeric excess was determined by normal phase HPLC analysis using Phenomonex Lux Cellulose-1 column (5 µm, 250 × 4.6 mm), eluent hexane/ethanol = 85/15, isocratic mode; 0.8 mL min^{-1} ; temperature 20 °C, UV detector 254 nm. Retention time for (*S*)-**16**: 16.1 min, for (*R*)-**16**: 17.6 min. Spectroscopic data are fully consistent with those reported in the literature [58].

(*S*)-(+)-2-(2-Nitro-1-phenylethyl)-1,3-diphenylpropane-1,3-dione (**18**): R$_f$: 0.35 (silica gel, hexane/EtOAc, 4:1); $[\alpha]_D^{25}$: +22.1 (DCM, *c* 1.0, 99.3% ee, *S* config.) (lit. $[\alpha]_D^{25}$: +21.3, DCM, *c* 1.0, 98% ee, *S* config. [59]); White crystals. Mp. 136.2 °C (lit. Mp: 135.6 °C [60]); MS-ESI+ (m/z): [M + H]$^+$ 391.2; When **Hub¹⁻⁴-cinchonas** were used as catalysts, enantiomeric excess was determined by reversed phase HPLC analysis using Phenomenex Lux Cellulose-1 column (5 µm, 250 × 4.6 mm), eluent water (0.1 % NH$_4$OAc)/MeCN = 30/70, isocratic mode; 0.8 mL·min^{-1}, temperature 20 °C, UV detector 222 nm. Retention time for (*S*)-**18**: 7.6 min, for (*R*)-**18**: 8.9 min. When hydroquinine (**1**) was used as a catalyst, enantiomeric excess value was determined by normal phase HPLC analysis with Kromasil® 5-Amycoat column (250 × 4.6 mm ID, 5 µm) using hexane/ethanol (85:15) eluent. Retention time for (*R*)-**18**: 19.2 min, for (*S*)-**18**: 26.1 min. Spectroscopic data are fully consistent with those reported in the literature [60].

3.3. Nanofiltration

Membrane separation was carried out in a crossflow nanofiltration rig with 53 cm² effective area (*A*), as described in the literature [61]. PolarClean, as a green solvent [62], was used for the filtration, and the applied pressure was 10 bar. Two independent measurements were carried out, and the presented results are mean values. Equations 1 and 2 were used to calculate the rejection and permeance after 24 h recirculation in the rig, respectively.

$$Rejection~[\%] = \left(1 - \frac{c_p}{c_f}\right) \times 100\%$$ Eq. 1

$$Flux~[L~m^{-2}~h^{-1}] = \frac{V}{A \cdot t}$$ Eq. 2

where c_p and c_f are the permeate and feed concentrations of the solutes, respectively; *V* is the permeate volume, while *t* is the time of solvent permeation through the membrane with certain membrane area (*A*).

5. Conclusions

Four structurally different C_3-symmetric cinchona organocatalysts were prepared, in which the catalytic units are covalently anchored to a trifunctional central core (hub). Depending on the immobilization site, we obtained compounds, either containing or lacking mono H-bond donor groups on the cinchona skeleton.

The catalytic activities of these size-enlarged molecules were tested in the hydroxyalkylation of indole and Michael addition reaction. While the parent hydroquinine was found to be an efficient catalyst for the Friedel–Crafts reaction of indole (up to 73% ee), the hub-cinchona catalysts showed significantly lower enantioselectivities, regardless of the solvent applied. The structure-selectivity correlations revealed that catalysts with more rigid and extensive spacers performed better, suggesting a disadvantageous interaction of the individual cinchona units. On the contrary, in Michael addition reaction the hub-cinchona catalyst showed increased selectivity compared to hydroquinine, which indicates the positive effect of the C_3-symmetric structure. Furthermore, **Hub³-cinchona** was also shown to provide enantioselectivities up to 96% ee, in the case of a bulkier substrate. Finally, membrane recovery of the size-enlarged organocatalysts using PolarClean alternative solvent was found to be straightforward thanks to their ~4-fold increase in size compared to hydroquinine.

Author Contributions:

Methodology, P.K., Z.F., S. N. and J.K.; synthesis of compounds, P.K., Z.F., S. N. and P.K.; determination of ee values by chiral HPLC measurements, P.B. and B.M.; performing NMR experiments, data analysis, Z.G.; performing MS measurements, data analysis, M.D. and B.T.; writing—original draft preparation, P.K.; writing—review and editing, J.K., Z.F., S.N., P.K., P.B. and P.H.; project administration, J.K.; funding acquisition, P.H. and J.K.; resources, P.H. and J.K.; supervision, J.K.

Conflicts of Interest: The authors declare no conflict of interest.

References

1.   Kamer, P.; Vogt, D.; Thybaut, J. W. *Contemporary Catalysis: Science, Technology, and Applications*, Gld. ed.; The Royal Society of Chemistry, 2017.
2.   Jacobsen, E. N.; Pfaltz, A.; Yamamoto, H. *Comprehensive Asymmetric Catalysis I - III (Comprehensive Overviews in Chemistry)*, 1st ed., Springer-Verlag Berlin Heidelberg, 1999.
3.   Moberg, C. C_3 Symmetry in Asymmetric Catalysis and Chiral Recognition. *Angew. Chem. Int. Ed.* **1998**, *37*, 248–268. https://doi.org/10.1002/(SICI)1521-3773(19980216)37:3<248::AID-ANIE248>3.0.CO;2-5

4.   Moberg, C. The Role of Symmetry in Asymmetric Catalysis. *Isr. J. Chem.* **2012**, *52*, 653–662.
https://doi.org/10.1002/ijch.201200020

5.   Gade, L. H.; Bellemin-Laponnaz, S. Exploiting Threefold Symmetry in Asymmetric Catalysis: The Case of Tris(oxazolinyl)ethanes ("Trisox"). *Chem. Eur. J.* **2008**, *14*, 4142–4152.
https://doi.org/10.1002/chem.200701990

6.   Gibson, S. E.; Castaldi, M. P. Applications of chiral C$_3$-symmetric molecules. *Chem. Commun.* **2006**, 3045–3062.
https://doi.org/10.1039/B602237E

7.   Rodríguez, L-I.; Roth, T.; Fillol, J. L.; Wadepohl, H.; Gade, L. H. The More Gold—The More Enantioselective: Cyclohydroaminations of γ-Allenyl Sulfonamides with Mono-, Bis-, and Trisphospholane Gold(I) Catalysts. *Chem. Eur. J.* **2012**, *18*, 3721–3728.
https://doi.org/10.1002/chem.201103140

8.   Yamanaka, M.; Nakagawa, T.; Aoyama, R.; Nakamura, T. Synthesis and estimation of gelation ability of C$_3$-symmetry tris-urea compounds. *Tetrahedron*, **2008**, *64*, 11558–11567.
https://doi.org/10.1016/j.tet.2008.10.036

9.   Crisan, C. V.; Soran, A.; Bende, A.; Hàdade, N. D.; Terec, A.; Grosu, I. Synthesis, Structure and Supramolecular Properties of a Novel C3 Cryptand with Pyridine Units in the Bridges. *Molecules* **2020**, *25*, 3789.
https://doi.org/10.3390/molecules25173789

10.   Yu, M-H.; Liu, X-T.; Space, B.; Chang, Z.; Bu, X-H. Metal-organic materials with triazine-based ligands: From structures to properties and applications. *Coord. Chem. Rev.* **2021**, *427*, 213518.
https://doi.org/10.1016/j.ccr.2020.213518

11.   García, A.; Insuasty, B.; Herranz, M. A.; Martínez-Álvarez, R.; Martín, N. New Building Block for C$_3$ Symmetry Molecules: Synthesis of s-Triazine-Based Redox Active Chromophores. *Org. Lett.* **2009**, *11*, 5398–5401.
https://doi.org/10.1021/ol902203t

12.   Burns, B.; King, N. P.; Tye, H.; Studley, J. R.; Gamble, M.; Wills, M. Chiral phosphinamides: new catalysts for the asymmetric reduction of ketones by borane. *J. Chem. Soc., Perkin Trans. 1* **1998**, 1027–1038.
https://doi.org/10.1039/A709174E

13.   Du, D-M.; Fang, T.; Xu, J.; Zhang, S-W. Structurally Well-Defined, Recoverable C$_3$-Symmetric Tris(β-hydroxyphosphoramide)-Catalyzed Enantioselective Borane Reduction of Ketones. *Org Lett.* **2006**, *8*, 1327–1330.
https://doi.org/10.1021/ol0600584

14.   Han, J.; Wu, H.; Teng, M.; Li, Z.; Wang, Y.; Wang, L.; Pan, Y. Novel Tripod L-Prolinamide Catalysts Based on Tribenzyl- and Triphenylphosphine Oxide for the Direct Aldol Reaction. *Synlett* **2009**, *6*, 933–936.
https://doi.org/10.1055/s-0028-1087958

15.   Moorthy, J. N.; Saha, S. C$_3$-Symmetric Proline-Functionalized Organocatalysts: Enantioselective Michael Addition Reactions. *Eur. J. Org. Chem.* **2010**, 6359–6365.
https://doi.org/10.1002/ejoc.201000569

16.   Murai, K.; Fukushima, S.; Hayashi, S.; Takahara, Y.; Fujioka, H. C$_3$-Symmetric Chiral Trisimidazoline: Design and Application to Organocatalyst. *Org. Lett.* **2010**, *12*, 964–966.
https://doi.org/10.1021/ol902958m

17.   Murai, K.; Fukushima, S.; Nakamura, A.; Shimura, M.; Fujioka, H. C$_3$-Symmetric chiral trisimidazoline: the role of a third imidazoline and its application to the nitro Michael reaction and the α-amination of β-ketoesters. *Tetrahedron* **2011**, *67*, 4862–4868.
https://doi.org/10.1016/j.tet.2011.05.005

18.   Murai, K.; Nakamura, A.; Matsushita, T.; Shimura, M.; Fujioka, H. C$_3$-Symmetric Trisimidazoline-Catalyzed Enantioselective Bromolactonization of Internal Alkenoic Acids. *Chem. Eur. J.* **2012**, *18*, 8448–8453.
https://doi.org/10.1002/chem.201200647

19.   Takizawa, S.; Sako, M.; Abozeid, M. A.; Kishi, K.; Wathsala, H. D. P.; Hirata, S.; Murai, K.; Fujioka, H.; Sasai, H. Enantio- and Diastereoselective Betti/aza-Michael Sequence: Single Operated Preparation of Chiral 1,3-Disubstituted Isoindolines. *Org. Lett.* **2017**, *19*, 5426–5429.
https://doi.org/10.1021/acs.orglett.7b02693

20.   Boratyński, P. J. Dimeric Cinchona alkaloids. *Mol. Divers.* **2015**, *19*, 385–422.
https://doi.org/10.1007/s11030-014-9563-1

21.   Park, H-G.; Jeong, B-S.; Yoo, M-S.; Park, M-K.; Huh, H.; Jew, S-S. Trimeric *Cinchona* alkaloid phase-transfer catalyst: α,α,α-tris[*O*(9)-allylcinchonidinium]mesitylene tribromide. *Tetrahedron Lett.* **2001**, *42*, 4645–4648.
https://doi.org/10.1016/S0040-4039(01)00809-7

22.   Siva, A.; Murugan, E. A New Trimeric Cinchona Alkaloid as a Chiral Phase-Transfer Catalyst for the Synthesis of Asymmetric α-Amino Acids. *Synthesis* **2005**, *17*, 2927–2933.
https://doi.org/10.1055/s-2005-872170

23.   Siva, A.; Murugan, E. New trimeric Cinchona alkaloid-based quaternary ammonium salts as efficient chiral phase transfer catalysts for enantioselective synthesis of α-amino acids. *J. Mol. Catal. A Chem.* **2006**, *248*, 1–9.
https://doi.org/10.1016/j.molcata.2005.11.039

24.   Sivamani, J.; Duraimurugan, K.; Arockiam, J. B.; Paulpandian, S.; Balasaravanan, R.; Siva, A. Highly Enantioselective Asymmetric Michael Addition Reactions with New Chiral Multisite Phase-Transfer Catalysts. *Synlett* **2014**, *25*, 1685–1691. https://doi.org/10.1055/s-0033-1339124

25.   Beneto, A. J.; Sivamani, J.; Ashokkumar, V.; Balasaravanan, R.; Duraimurugan, K.; Siva, A. Highly enantioselective Michael addition reactions with new trimeric chiral phase transfer catalysts. *New J. Chem.* **2015**, *39*, 3098–3104. https://doi.org/10.1039/C4NJ02395A

26.   Károlyi, B. K.; Bősze, S.; Orbán, E.; Sohár, P.; Drahos, L.; Gál, E.; Csámpai, A. Acylated *mono-*, *bis-* and *tris-* Cinchona-Based Amines Containing Ferrocene or Organic Residues: Synthesis, Structure and *in Vitro* Antitumor Activity on Selected Human Cancer Cell Lines. *Molecules* **2012**, *17*, 2316–2329. https://doi.org/10.3390/molecules17032316

27.   Min, C.; Han, X.; Liao, Z.; Wu, X.; Zhou, H-B.; Dong, C. C$_3$-Symmetrical Cinchonine-Squaramide as New Highly Efficient, and Recyclable Organocatalyst for Enantioselective Michael Addition. *Adv. Synth. Catal.* **2011**, *353*, 2715–2720. https://doi.org/10.1002/adsc.201100066

28.   Han, X.; Liu, B.; Zhou, H-B.; Dong, C. Enhanced efficiency of recyclable C$_3$-symmetric cinchonine-squaramides in the asymmetric Friedel–Crafts reaction of indoles with alkyl trifluoropyruvate. *Tetrahedron: Asymmetry* **2012**, *23*, 1332–1337. https://doi.org/10.1016/j.tetasy.2012.08.015

29.   Han, X.; Dong, C.; Zhou, H-B. C$_3$-Symmetric Cinchonine-Squaramide-Catalyzed Asymmetric Chlorolactonization of Styrene-Type Carboxylic Acids with 1,3-Dichloro-5,5-dimethylhydantoin: An Efficient Method to Chiral Isochroman-1-ones. *Adv. Synth. Catal.* **2014**, *356*, 1275–1280. https://doi.org/10.1002/adsc.201300915

30.   Lv, W.; Guo, C.; Dong, Z.; Tang, S.; Liu, B.; Dong, C. C$_3$-Symmetric cinchonine-squaramide as a recyclable efficient organocatalyst for tandem Michael addition–cyclisation of malononitrile and nitrovinylphenols. *Tetrahedron: Asymmetry* **2016**, *27*, 670–674. https://doi.org/10.1016/j.tetasy.2016.05.011

31.   Phuong, H. A. L.; Blanford, C. F.; Szekely, G. Reporting the unreported: the reliability and comparability of the literature on organic solvent nanofiltration. *Green Chem.* **2020**, *22*, 3397–3409. https://doi.org/10.1039/D0GC00775G

32.   Hu, J.; Kim, C.; Halasz, P.; Kim, J. F.; Kim, J.; Szekely, G. Artificial intelligence for performance prediction of organic solvent nanofiltration membranes. *J. Membr. Sci.* **2021**, *619*, 118513. https://doi.org/10.1016/j.memsci.2020.118513

33.   Phuong, H. A. L.; Cseri, L.; Whitehead, G. F. S.; Garforth, A.; Budd, P.; Szekely, G. Environmentally benign and diastereoselective synthesis of 2,4,5-trisubstituted-2-imidazolines. *RSC Adv.* **2017**, *7*, 53278–53289. https://doi.org/10.1039/C7RA11827A

34.   Dong, R.; Liu, R.; Gaffney, P. R. J.; Schaepertoens, M.; Marchetti, P.; Williams, C. M.; Chen, R.; Livingston, A. G. Sequence-defined multifunctional polyethers via liquid-phase synthesis with molecular sieving. *Nat. Chem.* **2019**, *11*, 136–145. https://doi.org/10.1038/s41557-018-0169-6

35.   Székely, G.; Schaepertoens, M.; Gaffney, P. R. J.; Livingston, A. G. Beyond PEG2000: Synthesis and Functionalisation of Monodisperse PEGylated Homostars and Clickable Bivalent Polyethyleneglycols. *Chem. Eur. J.* **2014**, *20*, 10038–10051. https://doi.org/10.1002/chem.201402186

36.   Razali, M.; Didaskalou, C.; Kim, J. F.; Babaei, M.; Drioli, E.; Lee, Y. M.; Szekely, G. Exploring and Exploiting the Effect of Solvent Treatment in Membrane Separations. *ACS Appl. Mater. Interfaces* **2017**, *9*, 11279–11289. https://doi.org/10.1021/acsami.7b01879

37.   Voros, V.; Drioli, E.; Fonte, C.; Szekely, G. Process Intensification via Continuous and Simultaneous Isolation of Antioxidants: An Upcycling Approach for Olive Leaf Waste. *ACS Sustainable Chem. Eng.* **2019**, *7*, 18444–18452. https://doi.org/10.1021/acssuschemeng.9b04245

38.   Alammar, A.; Park, S.-H.; Williams, C. J.; Derby, B.; Szekely, G. Oil-in-water separation with graphene-based nanocomposite membranes for produced water treatment. *J. Membr. Sci.* **2020**, *603*, 118007. https://doi.org/10.1016/j.memsci.2020.118007

39.   Keraani, A.; Nasser, G.; Shahane, S.; Renouard, T.; Bruneau, C.; Rabiller-Baudry, M.; Fischmeister, C. Syntheses and characterization of molecular weight enlarged olefin metathesis pre-catalysts. *C. R. Chimie* **2017**, *20*, 717–723. https://doi.org/10.1016/j.crci.2017.01.001

40.   Kisszékelyi, P.; Nagy, S.; Fehér, Z.; Huszthy, P.; Kupai, J. Membrane-Supported Recovery of Homogeneous Organocatalysts: A Review. *Chemistry* **2020**, *2*, 742–758. https://doi.org/10.3390/chemistry2030048

41.   Siew, W. E.; Ates, C.; Merschaert, A.; Livingston, A. G. Efficient and productive asymmetric Michael addition: development of a highly enantioselective quinidine-based organocatalyst for homogeneous recycling via nanofiltration. *Green Chem.* **2013**, *15*, 663–674. https://doi.org/10.1039/C2GC36407G

42.   Shao, Z.; Zhang, H. Combining transition metal catalysis and organocatalysis: a broad new concept for catalysis. *Chem. Soc. Rev.* **2009**, *38*, 2745–2755. https://doi.org/10.1039/B901258N

43.   Zhong, C.; Shi, X. When Organocatalysis Meets Transition-Metal Catalysis. *Eur. J. Org. Chem.* **2010**, *2010*, 2999–3025. https://doi.org/10.1002/ejoc.201000004

44.   Didaskalou, C.; Kupai, J.; Cseri, L.; Barabas, J.; Vass, E.; Holtzl, T.; Szekely, G. Membrane-Grafted Asymmetric Organocatalyst for an Integrated Synthesis–Separation Platform. *ACS Catal.* **2018**, *8*, 7430–7438. https://doi.org/10.1021/acscatal.8b01706

45.   Schaepertoens, M.; Didaskalou, C.; Kim, J. F.; Livingston, A. G.; Szekely, G. Solvent recycle with imperfect membranes: A semi-continuous workaround for diafiltration. *J. Membr. Sci.* **2016**, *514*, 646–658. https://doi.org/10.1016/j.memsci.2016.04.056

46.   Zhao, D.; Kim, J. F.; Ignacz, G.; Pogany, P.; Lee, Y. M.; Szekely, G. Bio-Inspired Robust Membranes Nanoengineered from Interpenetrating Polymer Networks of Polybenzimidazole/ Polydopamine. *ACS Nano* **2019**, *13*, 125−133. https://doi.org/10.1021/acsnano.8b04123

47.   Ignacz, G.; Fei, F.; Szekely, G. Ion-Stabilized Membranes for Demanding Environments Fabricated from Polybenzimidazole and Its Blends with Polymers of Intrinsic Microporosity. *ACS Appl. Nano Mater.* **2018**, *1*, 6349–6356. https://doi.org/10.1021/acsanm.8b01563

48.   Cassani, C.; Martín-Rapún, R.; Arceo, E.; Bravo, F.; Melchiorre, P. *Nat. Protoc.* **2013**, *8*, 325–344. https://doi.org/10.1038/nprot.2012.155

49.   Zielińska-Błajet, M.; Kucharska, M.; Skarzewski, J. *Synthesis* **2006**, *2006*, 1176–1182. https://doi.org/10.1055/s-2006-926382

50.   Yaegashi, K.; Mikami, M. JP 2010024173 (20100204), 2010.

51.   Heidelberger, M.; Jacobs, W. A. Synthesis in the Cinchona Series. I. The Simpler Cinchona Alkaloids and Their Dihydro Derivatives. *J. Am. Chem. Soc.* **1919**, *41*, 817–833. https://doi.org/10.1021/ja02226a015

52.   Brandes, S.; Niess, B.; Bella, M.; Prieto, A.; Overgaard, J.; Jørgensen, K. A. Non-Biaryl Atropisomers in Organocatalysis. *Chem. Eur. J.* **2006**, *12*, 6039–6052. https://doi.org/10.1002/chem.200600495.

53.   Braje, W. M.; Frackenpohl, J.; Schrake, O.; Wartchow, R.; Beil, W.; Hoffmann, H. M. R. Synthesis of 10,11-DidehydroCinchona Alkaloids and Key Derivatives. *Helv. Chim. Acta* **2000**, *83*, 777–792. https://doi.org/10.1002/(SICI)1522-2675(20000412)83:4<777::AID-HLCA777>3.0.CO;2-W.

54.   Song, Y.; Kohlmeir, E. K.; Meade, T. J. Synthesis of Multimeric MR Contrast Agents for Cellular Imaging. *J. Am. Chem. Soc.* **2008**, *130*, 6662–6663. https://doi.org/10.1021/ja0777990.

55.   Gilbert, E. E.; Voreck, W. E. Evaluation of a New Organic Azide: Hexakis(Azidomethyl)Benzene (HAB). Propellants. *Explos. Pyrotech.* **1989**, *14*, 19–23. https://doi.org/10.1002/prep.19890140105.

56.   Lyle, M. P. A.; Draper, N. D.; Wilson, P. D. Enantioselective Friedel−Crafts Alkylation Reactions Catalyzed by a Chiral Nonracemic C2-Symmetric 2,2'-Bipyridyl Copper(II) Complex. *Org. Lett.* **2005**, *7*, 901–904. https://doi.org/10.1021/ol050075d

57.   Török, B.; Abid, M.; London, G.; Esquibel, J.; Török, M.; Mhadgut, S. C.; Yan, P.; Prakash, G. K. S. Highly Enantioselective Organocatalytic Hydroxyalkylation of Indoles with Ethyl Trifluoropyruvate. *Angew. Chem. Int. Ed.* **2005**, *44*, 3086–3089. https://doi.org/10.1002/anie.200462877.

58.   Evans, D. A.; Mito, S.; Seidel, D. Scope and Mechanism of Enantioselective Michael Additions of 1,3-Dicarbonyl Compounds to Nitroalkenes Catalyzed by Nickel(II)-Diamine Complexes. *J. Am. Chem. Soc.* **2007**, *129*, 11583–11592. https://doi.org/10.1021/ja0735913.

59.   Tan, B.; Zhang, X.; Chua, P. J.; Zhong, G. Recyclable Organocatalysis: Highly Enantioselective Michael Addition of 1,3-Diaryl-1,3-Propanedione to Nitroolefins. *Chem. Commun.* **2009**, 779–781. https://doi.org/10.1039/B813915F.

60.   Gönczi, K.; Kudar, V.; Jászay, Z.; Bombicz, P.; Faigl, F.; Madarász, J. Solid State Structural Relation and Binary Melting Phase Diagram of (S-) and Racemic 2-(2-Nitro-1-Phenylethyl)-1,3-Diphenyl-Propane-1,3-Dione. *Thermochim. Acta* **2014**, *580*, 46–52. https://doi.org/10.1016/j.tca.2014.01.028.

61.   Fei, F.; Phuong, H. A. L.; Blanford, C. F.; Szekely, G. Tailoring the Performance of Organic Solvent Nanofiltration Membranes with Biophenol Coatings. *ACS Appl. Polym. Mater.* **2019**, *1*, 452−460. https://doi.org/10.1021/acsapm.8b00161

62.   Cseri, L.; Szekely, G. Towards cleaner PolarClean: efficient synthesis and extended applications of the polar aprotic solvent methyl 5-(dimethylamino)-2-methyl-5-oxopentanoate. *Green Chem.* **2019**, *21*, 4178–4188. https://doi.org/10.1039/C9GC01958H